Foundations of Physics, Vol. 18, No. 10, 1988

Area in Phase Space as Determiner of Transition Probability: Bohr–Sommerfeld Bands, Wigner Ripples, and Fresnel Zones

W. Schleich,[1,2] H. Walther,[1,3] and J. A. Wheeler[2]

Received September 2, 1987

We consider an oscillator subjected to a sudden change in equilibrium position or in effective spring constant, or both—to a "squeeze" in the language of quantum optics. We analyze the probability of transition from a given initial state to a final state, in its dependence on final-state quantum number. We make use of five sources of insight: Bohr–Sommerfeld quantization via bands in phase space, area of overlap between before-squeeze band and after-squeeze band, interference in phase space, Wigner function as quantum update of B–S band and near-zone Fresnel diffraction as mockup Wigner function.

We join the larger community to salute David Bohm on his special birthday, celebrate his many contributions to physics—*solid* physics—including his much used *Quantum Theory*, his instructive version of the EPR experiment, and the famous Aharonov–Bohm effect. David Bohm has always been interested in the correspondences—and differences—between the predictions of classical and quantum mechanics. We discuss here one physical effect that shows the relation between the two approaches in an especially illuminating way: transition probability in its dependence on quantum number when an oscillator is subjected to a sudden change in equilibrium position, or effective spring constant, or both—subjected to what in the realm of quantum optics is known as a "squeeze." We discuss the probability of transition from before-squeeze state to after-squeeze state by five sources of insight: (1) The early Bohr–Sommerfeld (B–S)

[1] Max-Planck-Institut für Quantenoptik, D-8046 Garching bei München, West Germany.
[2] Department of Physics, University of Texas at Austin, Austin, Texas 78712.
[3] Sektion Physik der Universität München, D-8046 Garching bei München, West Germany.

0015-9018/88/1000-0953$06.00/0

idealization of quantum state as corresponding to a band of area h in phase space; (2) the area of *overlap* (measured in units h) between *the* before-squeeze band and *an* after-squeeze band (measured in units h) as one factor that governs jump probability; (3) the square of the cosine of the area (this time in units of $\hbar$) *caught* between the center lines of the two bands as consequence of an *interference in phase space* (different from but analogous to the familiar Young double-slit interference); (4) a typical Wigner function, a quantity analogous to probability in phase space, as quantum update of the B–S bands; (5) near-zone Fresnel diffraction as replicator of some of the features of the Wigner function.

The harmonic oscillator provides a description of the amplitude of one mode of the electromagnetic field and is a powerful source of insight on what is measurable and what not.[1] A massive cylinder rolling under the influence of gravity on a metal ruler bent into the shape of a parabola can serve as a model for the field oscillator. To begin with, the oscillator is in its lowest quantum state[2]

$$\psi_0(x) = \pi^{-1/4} \exp\{-\tfrac{1}{2}x^2\}$$

as expressed in terms of an appropriately normalized oscillator coordinate x.

A coherent state[3] is obtained from this ground state by a sudden displacement. In the mechanical model this is achieved by suddenly displacing the origin of the harmonic potential by an amount $x_0 = \sqrt{2}\alpha$ and lowering the potential energy by $\frac{1}{2}x_0^2 = \alpha^2$. The wavefunction of the state—so prepared—a coherent state reads

$$\psi_{\text{coh}}(x) = \pi^{-1/4} \exp\{-\tfrac{1}{2}(x - \sqrt{2}\alpha)^2\} \tag{1}$$

The displacement has altered the energy of the oscillator, by an amount $\frac{1}{2}x_0^2 = \alpha^2$. However, the energy distribution for the coherent state is not a delta function located at this classical value α^2. Instead there exists a Poissonian distribution[2] of probabilities

$$W_m = \left| \int_{-\infty}^{\infty} dx\, u_m(x)\, \psi_{\text{coh}}(x) \right|^2 = \frac{(\alpha^2)^m}{m!} e^{-\alpha^2} \tag{2}$$

that the oscillator is in its mth energy eigenstate[2,3]

$$u_m(x) = \pi^{-1/4}(2^m m!)^{-1/2} H_m(x) e^{-1/2x^2}$$

Here H_m denotes the mth Hermite polynomial.[4] In the language of quantized electromagnetic fields the Poissonian W_m shown in Fig. 1 by the solid curve represents the probability of finding m photons in a coherent state.

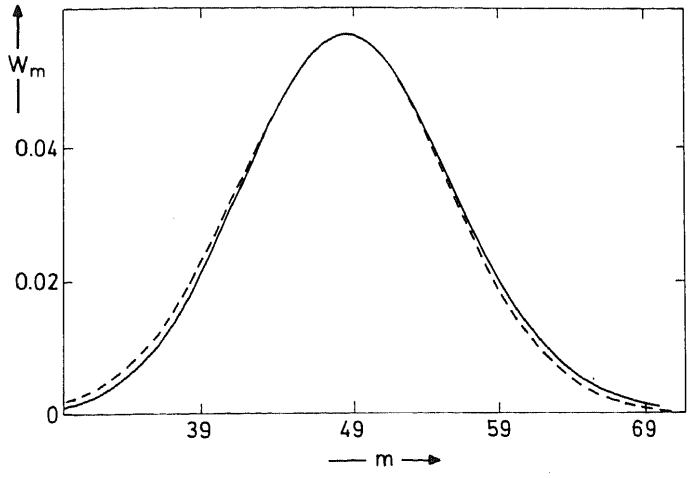

Fig. 1. The probability W_m of finding m photons in a coherent state is given by a Poisson distribution (solid line, Eq. (2)). This exact distribution and its asymptotic limit for large displacements (broken line, Eq. (3)) are almost indistinguishable in the neighborhood of the maximum, $m \cong \alpha^2 - \frac{1}{2}$. (We have chosen a displacement $\alpha = 7$. Every classical oscillator initially at rest and then subjected to such a displacement will undergo the same, sudden increase in energy, an increase which in our units is $\alpha^2 = 49$.) Curves, it should be recognized, are not curves, because m is never other than an integer.

In the limit of large displacements, that is $\alpha^2 \gg 1$, the Poissonian Eq. (2) allows (Appendix A) the asymptotic expansion

$$W_m = \frac{1}{\sqrt{2\pi\alpha}} \exp\left\{ -\left[\frac{m + \frac{1}{2} - \alpha^2}{\sqrt{2}\alpha} \right]^2 \right\} \tag{3}$$

depicted in Fig. 1 by the broken line.

What is a *natural* algorithm for estimating the transition probabilities W_m of Eq. (3)? Certainly the quantum mechanical scalar product of Eq. (2) is an excellent *mathematical* tool for this purpose but does not provide any insight into the physics.

The most immediate source of physical insight comes from Bohr's correspondence principle[5] and semiclassical quantum mechanics:[6] "Bohr's Zauberstab," or Bohr's magic wand in the language of Sommerfeld.[7] That picture leads immediately to the concept of *area of overlap*—overlap between the two states represented as "bands" in phase space—*as determiner of transition probability.*[8,9]

The energy in the mth number state is

$$m + \tfrac{1}{2} = \tfrac{1}{2} p_m^2 + \tfrac{1}{2} x^2 \tag{4}$$

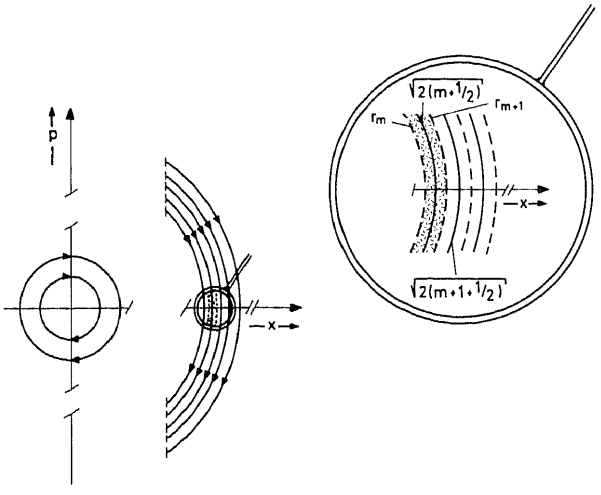

Fig. 2. A single mode of the electromagnetic field in a number state is equivalent to a harmonic oscillator with dimensionless variables x and p. The trajectories in phase space are circles with radius $\sqrt{2(m+1/2)}$. With each state we associate a band of area 2π (in units $\hbar$), defined by its inner radius $r_m=\sqrt{2m}$ and outer radius $r_{m+1}=\sqrt{2(m+1)}$.

and the trajectories in phase space are circles of radius $\sqrt{2(m+1/2)}$. Each state takes up an area 2π in phase space.[10] We therefore associate with the mth number state an occupied band of inner radius $\sqrt{2m}$ and outer radius $\sqrt{2(m+1)}$ as shown in Fig. 2.

The coherent state is a displaced ground state ($m=0$), and according to Eq. (4) can thus be represented in its simplest version as a circle of radius unity

$$1=p_{\mathrm{coh}}^2+(x-\sqrt{2}\alpha)^2 \tag{5}$$

centered at $x_0=\sqrt{2}\alpha$ on the positive x axis as indicated in Fig. 3.

The area of overlap A_m between the mth occupied Bohr–Sommerfeld band and the circle, Eq. (5), is thus

$$A_m=\int\limits_{\substack{\text{overlap } m\text{th band}\\ \text{coherent state}}} dx\int dp\ \frac{1}{\pi} \tag{6}$$

where we have introduced the factor π^{-1} to maintain the normalization condition

$$\sum_m A_m=\frac{1}{\pi}\sum_m \int\limits_{\substack{\text{overlap } m\text{th band}\\ \text{coherent state}}} dx\int dp\ =\frac{1}{\pi}\cdot\begin{pmatrix}\text{area of coherent}\\ \text{state}=\pi\end{pmatrix}=1$$

What does this algorithm yield for W_m? For m values either smaller or larger than two critical values, that is, for $\sqrt{2(m+1/2)} \lesssim \sqrt{2}\alpha - 1$ and for $\sqrt{2}\alpha + 1 \lesssim \sqrt{2(m+1/2)}$, the bands and the circle do not overlap at all and thus

$$W_m = 0$$

Bands corresponding to m values between these critical values have an area

$$A_m \cong \frac{1}{\pi}(\sqrt{2(m+1)} - \sqrt{2m})\, 2p_{\text{coh}}[\tfrac{1}{2}(\sqrt{2(m+1)} + \sqrt{2m})] \tag{7}$$

in common with the circle. Here we have approximated the area of the mth ring segment by the area of a rectangle of width, $\Delta_m \equiv \sqrt{2(m+1)} - \sqrt{2m}$ and height, $2p_{\text{coh}}$ evaluated at the center of the band. In Bohr's semiclassical limit, $m \gg 1$, the width, Δ_m, becomes

$$\Delta_m \cong \sqrt{2m}\left(1 + \frac{1}{2}\frac{1}{m} - \frac{1}{8}\frac{1}{m^2} - 1\right) \cong \frac{1}{\sqrt{2(m+\frac{1}{2})}} \cong \frac{1}{\sqrt{2}\alpha} \tag{8}$$

With the help of this result and Eq. (5) the expression for the area reduces to

$$A_m \cong \frac{1}{\pi\alpha}\sqrt{2}\{1 - [\tfrac{1}{2}(\sqrt{2(m+1)} + \sqrt{2m}) - \sqrt{2}\alpha]^2\}^{1/2} \tag{9}$$

In the large m limit we have

$$\tfrac{1}{2}(\sqrt{2(m+1)} + \sqrt{2m}) - \sqrt{2}\alpha \cong \sqrt{2(m+\tfrac{1}{2})} - \sqrt{2}\alpha \cong \frac{m + \frac{1}{2} - \alpha^2}{\sqrt{2}\alpha} \tag{10}$$

In this limit Eq. (9) simplifies to

$$A_m \cong \frac{1}{\pi\alpha^2}\{2\alpha^2 - (m + \tfrac{1}{2} - \alpha^2)^2\}^{1/2} \tag{11}$$

The tentative probability distribution, $W_m = A_m$ is thus peaked at $m = \alpha^2 - \frac{1}{2}$ and has the half width $\sqrt{2}\alpha$, in agreement with Eq. (3). In this approach each point inside the coherent state circle carries equal weight resulting in the square root dependence of W_m on m.

A better treatment recognizes the smooth spread in x values

$$|\psi_{\text{coh}}(x)|^2 = \pi^{-1/2} \exp\{-(x - \sqrt{2}\alpha)^2\}$$

and (by Fourier analysis) the corresponding spread in momentum

$$|\phi_{\text{coh}}(p)|^2 = \pi^{-1/2} \exp\{-p^2\}$$

Thus each point in phase space gets weighted according to the Wigner–Cohen distribution[11]

$$P_{\mathrm{coh}}^{(W)}(x, p) = \pi^{-1} \exp\{-(x - \sqrt{2}\alpha)^2 - p^2\} \tag{12}$$

and the circular spot shown in Fig. 3 crudely depicts the exponential fall-off of the distribution—an effect analogous to the apodization, for a smooth graduation in transmissivity, often used to improve a lens.

An improved version of the area-of-overlap concept therefore evaluates the overlap $\mathcal{A}_m$ between the mth band and the Gaussian bell

$$\mathcal{A}_m = \int_{m\text{th band}} dx \int dp \; P_{\mathrm{coh}}^{(W)}(x, p)$$

In the limit $m \gg 1$ we find for $\mathcal{A}_m$, approximated by the mth, weighted rectangle

$$\mathcal{A}_m \cong \Delta_m \exp\{-[\tfrac{1}{2}(\sqrt{2(m+1)} + \sqrt{2m}) - \sqrt{2}\alpha]^2\} \frac{1}{\pi} \int_{-\infty}^{\infty} dp \, e^{-p^2} \tag{13}$$

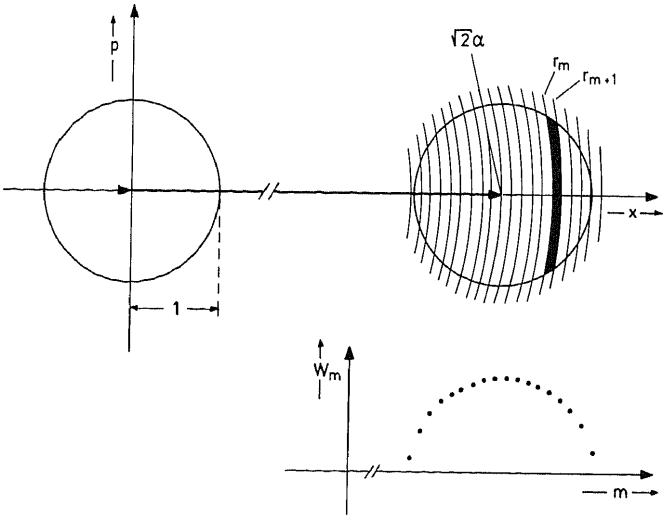

Fig. 3. The ground state of a harmonic oscillator, visualized in phase space as a circle of radius unity and displaced from the origin by an amount $\sqrt{2}\alpha$ models a coherent state. The area of overlap between the mth band (representing the mth number state) and the circle, the simplest algorithm for determining the photon distribution W_m of a coherent state, yields a "semi-ellipse shaped" distribution, Eq. (11), reproducing the qualitative features of the Poisson distribution, as shown in the lower right. When instead we weight each point of phase space according to the circular Gaussian $P_{\mathrm{coh}}^{(W)}$ (Eq. (12)) we get a probability distribution, W_m, in m values (Eq. (3), depicted in Fig. 1 by the broken line) almost indistinguishable from the correct Poissonian result, Eq. (2).

which with the help of Eqs. (8) and (10) reduces to

$$\mathcal{A}_m \cong \frac{1}{\sqrt{2\pi\alpha}} \exp\left\{-\left[\frac{m+\frac{1}{2}-\alpha^2}{\sqrt{2}\alpha}\right]^2\right\} = W_m$$

a result identical to Eq. (3).

In the semiclassical limit the photon statistics of a coherent state, W_m, can therefore be understood as the overlap in phase space between the Gaussian bell of the coherent state and the corresponding Bohr–Sommerfeld band of the mth number state.

This concept of *area of overlap in phase space as a determiner of transition probability* can be made precise by replacing the bands of the Bohr–Sommerfeld scheme of quantization by the corresponding Wigner functions. In this formulation the probability, W_m, of Eq. (2) is given[11,12] by

$$W_m = 2\pi \int_{-\infty}^{\infty} dx \int_{-\infty}^{\infty} dp\, P_m^{(W)}(x, p)\, P_{\mathrm{coh}}^{(W)}(x, p) \tag{14}$$

The Wigner function, $P_m^{(W)}$ of the harmonic oscillator[11,13] in its mth state of excitation reads

$$P_m^{(W)}(x, p) = \frac{(-1)^m}{\pi} \exp\{-(x^2+p^2)\}\, L_m[2(x^2+p^2)] \tag{15}$$

where L_m denotes the mth Laguerre polynomial.[4] This quantity is plotted in Fig. 4 for $m = 10$. The distribution has radial symmetry. The mth Laguerre polynomial has m real zeros. Thus the phase space is divided into $m+1$ bands with alternating signs. In other words, neighboring bands have a phase difference π. Moreover, the function $e^{-\xi/2}L_m(\xi)$ has a turning point[14] for $\xi \equiv 2(x^2+p^2) \cong 4(m+1/2)$. Therefore, the outermost band is located in the neighborhood of the Bohr–Sommerfeld phase space trajectory of Eq. (4). The prefactor $(-1)^m$ in Eq. (15) ensures that the Wigner function at this outermost band has positive values. In addition, the integrated probability for this one band alone is approximately unity as shown in Appendix B. The outermost Wigner band thus is the sophisticated version of the familiar Bohr–Sommerfeld band of Fig. 2, in full accord with Bohr's correspondence principle.

The probability, W_m, of finding m photons in a coherent state is given by the overlap in phase space between the Wigner function of the coherent state shown in Fig. 5a and the distribution function of the harmonic oscillator in its mth state shown in Fig. 5b. In order to make contact with and stress the analogy to the area-of-overlap approach we again perform

the phase space integration of Eq. (14) in the limit of large displacements; that is, $\alpha^2 \gg 1$. The general treatment can be found in Appendix C.

Again the exponential fall-off of the Gaussian bell of the coherent state confines the phase space integration to a circular spot of radius unity centered at $x = \sqrt{2}\alpha \gg 1$ as shown in Fig. 5c. Moreover Fig. 5b demonstrates that similar to the Bohr–Sommerfeld bands the ripples in phase space of the Wigner function are, at least in the neighborhood of the coherent state, "plane waves." This translates itself into

$$e^{-(x^2+p^2)} L_m[2(x^2+p^2)] \cong e^{-x^2} L_m(2x^2)$$

which allows to decouple the x and p integration in Eq. (14),

$$W_m \cong \left(2\int_{-\infty}^{\infty} dx\, e^{-(x-\sqrt{2}\alpha)^2}(-1)^m e^{-x^2} L_m(2x^2)\right)\frac{1}{\pi}\int_{-\infty}^{\infty} dp\, e^{-p^2} \quad (16)$$

Since in the neighborhood of $x \cong \sqrt{2}\alpha$ the Gaussian is slowly varying the contributions from consecutive wave fronts will average out, except for the outermost band located at $x \cong \sqrt{2(m+1/2)}$. The integral over x in Eq. (16)

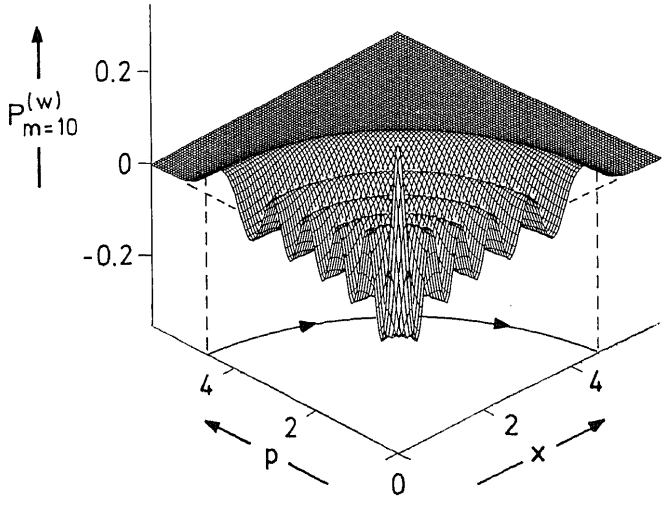

Fig. 4. The Wigner function of a harmonic oscillator in its $m = 10$th state of excitation consists of $m+1 = 11$ spherical wave fronts emerging from the origin much as water waves originate from a stone thrown into the water. Neighboring fronts have a phase difference of π; that is, the Wigner function alternates m times between positive and negative values. The location of the outermost wave front is governed by the quantized phase space trajectory $x^2 + p^2 = 2(m+1/2)$.

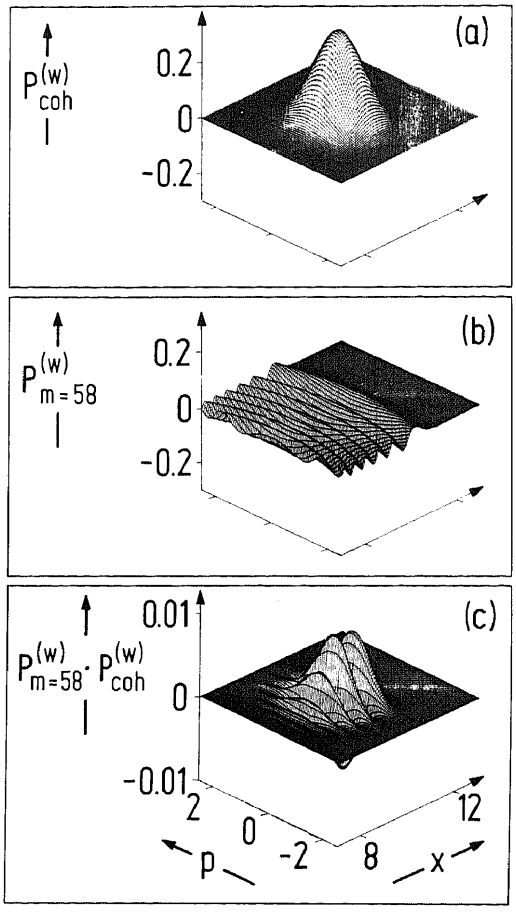

Fig. 5. In the framework of the Wigner distribution function, the probability $W_{m=58}$ of finding $m=58$ photons in a coherent state is obtained by integrating the product of the Wigner function of the coherent state (a)—a Gaussian bell—and the Wigner function of the harmonic oscillator in its $m=58$-th state (b) over phase space. Due to the exponential fall-off of the Gaussian bell the ripples in phase space caused by the oscillator (b) only contribute within a circle of radius unity centered at $x=\sqrt{2}\alpha=\sqrt{2}\cdot 7$ as shown in (c). Within this circular spot, the wave fronts are essentially straight, that is, "plane waves"; and the contributions to W_m from consecutive wave fronts approximately compensate each other. The probability W_m is thus governed by the overlap between the bell and the outermost band located roughly at $x=\sqrt{2(m+1/2)}$ shown in (c) by the peak furthest to the right.

can therefore be approximated by evaluating the Gaussian at $x = \sqrt{2(m+1/2)}$ and by taking it out of the integral, that is

$$W_m \cong \left(2\int_{r_0}^{\infty} dx(-1)^m e^{-x^2} L_m(2x^2)\right) \exp\{-(\sqrt{2(m+1/2)} - \sqrt{2}\alpha)^2\} \times \left(\frac{1}{\pi}\int_{-\infty}^{\infty} dp\, e^{-p^2}\right) \tag{17}$$

where $\rho_0 \equiv 2r_0^2$ denotes the largest zero[4,14] of the mth Laguerre polynomial. As shown in Appendix B the remaining integration in the x variable yields the width, Δ_m, (Eq. (8)) of the mth Bohr–Sommerfeld band. Therefore, with the help of Eq. (10), Eq. (17) is identical to Eq. (13) and thus yields the Gaussian approximation, Eq. (3), of W_m.

We summarize the above considerations by emphasizing that due to their π-phase difference the inner wave fronts of the Wigner function of the harmonic oscillator do not contribute significantly to W_m. The outermost band, however, yields a contribution equivalent to a circular Bohr–Sommerfeld band of width Δ_m. Therefore, in this problem the Wigner function $P_m^{(W)}$ can be replaced[15] in its simplest version by the occupied B–S band of Fig. 2. Although the inner wave fronts do not contribute to the photon distribution, W_m, of a coherent state, they play an important role in the photon statistics of a highly squeezed state: They are the origin of the oscillatory behavior[8,16] of this photon count probability.

There exists a remarkable analogy between the area-of-overlap concept as applied to coherent states and Fresnel diffraction at a circular aperture.[17,18] Imagine an opaque shield containing a circular hole which is being illuminated by plane waves from a very distant point source. Consider a detector located in the near-field region; that is, at a distance from the aperture small in comparison with (aperature radius × reduced wavelength)$^{1/2}$. The diffracted electric field is governed by the Fresnel zones (radii proportional to the square root of m!) that appear in the circular aperture as shown by the insets in Fig. 6. On the other hand, we recall that the probability, W_m, of finding m photons in a coherent state is determined by the area of the mth band ($r_m \sim m^{1/2}$) that appears within the circular spot in Fig. 3. The displacement of the coherent state in *phase space* translates itself in the optical analog into a displacement of the point of observation, R, in *ordinary space* away from the center of the hole.

This analogy fails in one point. In the area-of-overlap algorithm the probability W_m is given by the overlap on the initial spot of *one* single band, namely the mth band. In contrast the diffracted electric field is determined by *interference* from *all* Fresnel zones that appear in the aperature, each having a relative phase difference of π.

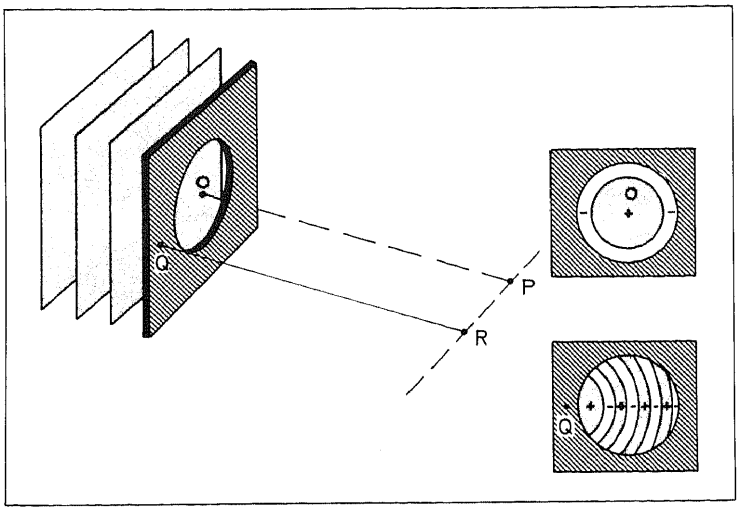

Fig. 6. The Fresnel-diffracted electric field at a point behind a screen with a circular hole which is illuminated by plane waves is the sum of contributions from the Fresnel zones that appear in the aperture as shown by the insets. Neighboring zones have the phase difference π. In the case of observation at P two complete zones are assumed to be present. When the point of observation P is displaced at R, only segments of the Fresnel zones with center Q play a role, a result analogous to the area-of-overlap approach of Fig. 3.

In summary, we explain the photon distribution of a coherent state geometrically as the overlap in phase space between the Bohr–Sommerfeld number state bands and the circular spot of the coherent state. We demonstrate that this formalism is equivalent to the corresponding precise Wigner function treatment in the large-quantum-number limit of Bohr's correspondence principle. The area-of-overlap concept shows elements reminiscent of Fresnel diffraction at a circular aperture: The Bohr–Sommerfeld–Wigner ripples are Fresnel zones in phase space appearing in the circular aperture of the coherent state.

ACKNOWLEDGMENTS

The authors thank L. Cohen, K. Dodson, M. Hillery, J. Kimble, K. Kraus, R. F. O'Connell, G. Rainer, and M. O. Scully for useful and stimulating discussions. In particular, we thank C.-S. Cha for the computer evaluation of the curves shown here. Preparation of this article was assisted by the University of Texas at Austin and by NSF Grant PHY 850 3890.

APPENDIX A: ASYMPTOTIC EXPANSION OF POISSON DISTRIBUTION

The Poisson distribution

$$W_m = \frac{\lambda^m}{m!} e^{-\lambda} \tag{A1}$$

shows the familiar Gaussian limit[19] for $\lambda \to \infty$,

$$W_m \cong (2\pi\lambda)^{-1/2} \exp\left\{-\left[\frac{m-\lambda}{\sqrt{2\lambda}}\right]^2\right\} \tag{A2}$$

Since for any integer value of λ,

$$W_{\lambda-1} = W_\lambda$$

the maximum of W_m is located at $\lambda - \frac{1}{2}$ in contrast to Eq. (A2). An improved approximation, valid at least in the neighborhood of $m = \lambda$, is therefore

$$W_m \cong (2\pi\lambda)^{-1/2} \exp\left\{-\left[\frac{m+\frac{1}{2}-\lambda}{\sqrt{2\lambda}}\right]^2\right\} \tag{A3}$$

as confirmed by Fig. 1.

We now derive Eq. (A3) based on the improved Stirling formula[20]

$$m! \cong (2\pi)^{1/2} \frac{(m+\frac{1}{2})^{m+1/2}}{e^{m+1/2}} \tag{A4}$$

From the logarithm of Eq. (A1)

$$\ln W_m = m \ln \lambda - \ln(m!) - \lambda$$

we find with the help of Eq. (A4)

$$\ln W_m = (m+\tfrac{1}{2}) \ln\left(\frac{\lambda}{m+\frac{1}{2}}\right) + m + \tfrac{1}{2} - \lambda - \ln(2\pi\lambda)^{1/2}$$

When we introduce $\delta \equiv m + \frac{1}{2} - \lambda$ the above equation reads

$$\ln W_m \cong (\lambda+\delta) \ln\left(1 - \frac{\delta}{\lambda+\delta}\right) + \delta - \ln(2\pi\lambda)^{1/2}$$

which for $\delta/\lambda \ll 1$ reduces to

$$\ln W_m \cong -\frac{1}{2}\frac{\delta^2}{\lambda} - \ln(2\pi\lambda)^{1/2}$$

a result equivalent to Eq. (A3).

APPENDIX B. AREA IN PHASE SPACE OCCUPIED BY OUTERMOST WIGNER BAND

In this Appendix we show that the area in phase space occupied by the outermost band of the Wigner function of a highly excited harmonic oscillator is approximately unity. We therefore calculate

$$I_m \equiv \int_{r_0}^{\infty} dr\, r \int_{-\pi}^{\pi} d\varphi \frac{(-1)^m}{\pi} e^{-r^2} L_m(2r^2)$$

where $\rho_0 \equiv 2r_0^2$ denotes the largest zero of the mth Laguerre polynomial.[4,14] When we perform the angular integration and introduce $\rho \equiv 2r^2$ we find

$$I_m \equiv \frac{(-1)^m}{2} \int_{\rho_0}^{\infty} d\rho\, e^{-\rho/2} L_m(\rho) \tag{B1}$$

With the help of[4,14]

$$L_m(\rho) = \frac{d}{d\rho} \{L_m(\rho) - L_{m+1}(\rho)\}$$

we integrate in Eq. (B1) by parts and deduce the following recurrence relation

$$I_{m+1} = I_m + (-1)^m e^{-\rho_0/2} [L_m(\rho_0) - L_{m+1}(\rho_0)] \tag{B2}$$

with the initial condition

$$I_0 = e^{-\rho_0/2} \tag{B3}$$

It is easy to show

$$I_m = 2e^{-\rho_0/2} \left\{ \sum_{k=0}^{m-1} (-1)^k L_k(\rho_0) + \frac{1}{2} (-1)^m L_m(\rho_0) \right\}$$

satisfies Eqs. (B2) and (B3).

In the limit of $m \to \infty$, we can perform the summation with the help of the generating function[4,14] of the Laguerre polynomials,

$$(1-\xi)^{-1} \exp\left\{\frac{\rho\xi}{\xi - 1}\right\} = \sum_{k=0}^{\infty} \xi^k L_k(\rho)$$

to find

$$I_m \cong 1 \tag{B4}$$

In the last step we have also made use of the fact that by definition, $e^{-\rho_0/2} L_m(\rho_0) = 0$

We now apply Eq (B4) to obtain an approximation for the integral

$$\Lambda_m \equiv 2 \int_{r_0}^{\infty} dx (-1)^m e^{-x^2} L_m(2x^2) = 2^{-1/2} \int_{\rho_0}^{\infty} d\rho \; \rho^{-1/2} (-1)^m e^{-\rho/2} L_m(\rho)$$

Since $\rho^{-1/2}$ is a slowly varying function in the neighborhood of the turning point of $(-1)^m e^{-\rho/2} L_m(\rho)$, that is at $\rho_t = 4(m + 1/2)$ we evaluate $\rho^{-1/2}$ at ρ_t which yields

$$\Lambda_m \cong \frac{1}{\sqrt{2(m+1/2)}} \cong \Lambda_m$$

Here we have made use of Eqs. (B4) and (8).

APPENDIX C: PHOTON DISTRIBUTION OF COHERENT STATES VIA WIGNER FUNCTIONS

In this Appendix we rederive the Poissonian photon distribution of a coherent state [Eq. (2)] in terms of Wigner functions. With the help of Eqs. (12) and (15), Eq. (14) reads

$$W_m = \frac{2(-1)^m}{\pi} e^{-2\alpha^2} \int_{-\infty}^{\infty} dx \int_{-\infty}^{\infty} dp \, e^{-2(x^2+p^2)} L_m[2(x^2+p^2)] e^{2\sqrt{2}\alpha x} \qquad \text{(C1)}$$

The integration over phase space is most conveniently achieved in polar coordinates

$$x = r \cos\varphi, \qquad p = r \sin\varphi$$

which reduce Eq. (C1) to

$$W_m = \frac{2(-1)^m}{\pi} e^{-2\alpha^2} \int_0^{\infty} dr \, r \int_{-\pi}^{\pi} d\varphi \, e^{-2r^2} L_m(2r^2) e^{2\sqrt{2}\alpha r \cos\varphi}$$

The familiar relation[21]

$$\frac{1}{2\pi} \int_{-\pi}^{\pi} d\varphi \, e^{2\sqrt{2}\alpha r \cos\varphi} = \mathcal{J}_0(i2\sqrt{2}\alpha r) = \mathcal{J}_0[2\sqrt{(2r^2)(-\alpha^2)}]$$

where $\mathcal{J}_0$ denotes the Bessel function of zeroth order, allows to perform the integration over the angle variable φ and with $\rho \equiv 2r^2$ we arrive at

$$W_m = (-1)^m e^{-2\alpha^2} \int_0^{\infty} d\rho \, e^{-\rho} L_m(\rho) \, \mathcal{J}_0[2\sqrt{\rho(-\alpha^2)}] \qquad \text{(C2)}$$

The generating function[4] of the Laguerre polynomials

$$\mathcal{J}_0(2\sqrt{\rho y}) = e^{-y} \sum_{k=0}^{\infty} \frac{y^k}{k!} L_k(\rho)$$

reduces Eq. (C2) to

$$W_m = (-1)^m e^{-\alpha^2} \sum_{k=0}^{\infty} \frac{(-\alpha^2)^k}{k!} \int_0^{\infty} d\rho\, e^{-\rho} L_m(\rho)\, L_k(\rho)$$

which, with the help of the orthonormalization property[4]

$$\int_0^{\infty} d\rho\, e^{-\rho} L_m(\rho)\, L_k(\rho) = \delta_{m,k}$$

yields the Poissonian, Eq. (2).

REFERENCES

1. See the classic papers by L. Landau and R. Peierls, *Z. Phys.* **69**, 56–69 (1931); N. Bohr and L. Rosenfeld, *Mat. Fys. Medd. Dan. Vid. Selsk.* **12**, no. 8 (1933) and N. Bohr and L. Rosenfeld, *Phys. Rev.* **78**, 794–798 (1950); these papers are reprinted and commented on in J. A. Wheeler and W. H. Zurek, eds., *Quantum Theory and Measurement* (Princeton University Press, Princeton, 1983).
2. D. Bohm, *Quantum Theory* (Prentice–Hall, Englewood Cliffs, 1951).
3. See, e.g., W. H. Louisell, *Quantum Statistical Properties of Radiation* (Wiley, New York, 1973), or in M. Sargent, M. O. Scully, and W. E. Lamb, Jr., *Laser Physics* (Addison-Wesley, Reading, 1974).
4. G. Szegö, *Orthogonal Polynomials* (American Mathematical Society, New York, 1939).
5. See, e.g., M. Born, *Vorlesungen über Atommechanik*, in *Struktur der Materie in Einzeldarstellungen*, M. Born and J. Franck, eds. (Springer, Berlin, 1925); P. Debye, *Physik. Z.* **28**, 170–174 (1927).
6. W. Pauli, *Die allgemeinen Prinzipien der Wellenmechanik*, in *Handbuch der Physik*, Vol. 24, H. Geiger and K. Scheel, eds. (Springer, Berlin, 1933), or H. A. Kramers, *Quantentheorie des Elektrons und der Strahlung*, Vol. 2 in *Hand- und Jahrbuch der Chemischen Physik* (Eucken–Wolf, Leipzig, 1938).
7. According to F. Hund (talk at the Tagung der Deutschen Physikalischen Gesellschaft, Göttingen, 1987), A. Sommerfeld referred to Bohr's correspondence principle during the Bohr Festspiele in Göttingen 1924 as "Bohrs Zauberstab."
8. For the application of the area-of-overlap concept to squeezed states, see, e.g., J. A. Wheeler, *Lett. Math. Phys.* **10**, 201–206 (1985); W. Schleich and J. A. Wheeler, *Nature* **326**, 574–577 (1987); W. Schleich and J. A. Wheeler, in *The Physics of Phase Space*, by Y. S. Kim and W. W. Zachary, eds. (Springer, New York, 1987), pp. 200–204; W. Schleich and J. A. Wheeler, *Verh. Deut. Phys. Ges. (VI)* **22**, a15.3 (1987); W. Schleich and J. A. Wheeler, *J. Opt. Soc. Am. B* **4**, 1715–1722 (1987).
9. A paper is in preparation by W. Schleich and J. A. Wheeler on the area-of-overlap concept as applied to Franck–Condon transitions in diatomic molecules.

10. A. Sommerfeld, *Sitzungsber. Münch. Akad. Wiss.* (1915) 425–458; *ibid.* 459–500; *Ann. Phys. (Leipzig)* **51**, 1–167 (1916); M. Planck, *Ann. Phys. (Leipzig)* **50**, 385–418 (1916); P. Ehrenfest, *Ann. Phys. (Leipzig)* **51**, 327–352 (1916).
11. See, e.g., the reviews by M. Hillery, R. F. O'Connell, M. O. Scully, and E. P. Wigner, *Phys. Rep.* **106**, 121–167 (1984); V. I. Tatarskii, *Usp. Fiz. Nauk.* **139**, 587–619 (1983) [*Sov. Phys. USPEKHI* **26**, 311–327 (1983)]; L. Cohen in *Frontiers of Nonequilibrium Statistical Physics*, G. Moore and M. O. Scully, eds. (Plenum, New York, 1986), pp. 97–117.
12. R. F. O'Connell and E. P. Wigner, *Phys. Lett.* **83A**, 145–148 (1981); R. F. O'Connell and A. K. Rajagopal, *Phys. Rev. Lett.* **48**, 525–526 (1982); R. F. O'Connell and D. F. Walls, *Nature* **312**, 257–258 (1984); for an application of this relation to molecular collisions, see H.-W. Lee and M. O. Scully, *J. Chem. Phys.* **73**, 2238–2242 (1980).
13. See, e.g., J. R. Klauder, *Bell Sys. Tech. J.* **39**, 809–820 (1960).
14. F. Tricomi, *Vorlesungen über Orthogonalreihen* (Springer, Berlin, 1955).
15. The semiclassical limit of the Wigner function has been considered in a multitude of publications; see, for example, E. J. Heller, *J. Chem. Phys.* **67**, 3339–3351 (1977); M. V. Berry, *Phil. Trans. Roy. Soc. (London)* **287**, 237–271 (1977); M. V. Berry and N. L. Balazs, *J. Phys.* **A12**, 625–642 (1979); H. J. Korsch, *J. Phys.* **A12**, 811–823 (1979); N. L. Balazs and B. K. Jennings, *Phys. Rep.* **104**, 347–391 (1984). It has been pointed out frequently that, for most cases, the Wigner function in the semiclassical limit can be expressed by an appropriately normalized delta function located at the Bohr–Sommerfeld phase space trajectory. For insight into when and why, see especially, J. P. Dahl, in *Energy Storage and Redistribution in Molecules*, J. Hinze, ed. (Plenum, New York, 1983), pp. 557–571, and J. P. Dahl, in *Semiclassical Descriptions of Atomic and Nuclear Collisions*, J. Bang and J. de Boer, eds. (Elsevier, Amsterdam, 1985), pp. 379–394.
16. W. Schleich, D. F. Walls, and J. A. Wheeler, *Phys. Rev. A* **38**, 1177–1186 (1988).
17. E. Hecht and A. Zajac, *Optics* (Addison-Wesley, Reading, 1980).
18. M. Born and E. Wolf, *Principles of Optics* (Pergamon Press, London, 1959).
19. See, e.g., S. Chandrasekhar, *Rev. Mod. Phys.* **15**, 1–89 (1943); reprinted in *Selected Papers on Noise and Stochastic Processes*, N. Wax, ed. (Dover, New York, 1954).
20. See, e.g., C. Leubner, *Eur. J. Phys.* **6**, 299–301 (1985) and references therein.
21. I. S. Gradshteyn and I. M. Ryzhik, *Table of Integrals, Series and Products* (Academic Press, New York, 1980)